Analysis of the Benefits of Superposition Coding in Random Wireless Networks

Sundaram Vanka* and Martin Haenggi

***Abstract*—Network-wide adoption of a multipacket transmission scheme such as Superposition Coding (SC) for local "one-to-many" communication results in mutually interfering "broadcast" clusters. We analyze the benefits of SC and traditional Frequency Division (FD) with this interference via a utility function that measures the rate of information transfer per unit area. In particular, we study transmitters forming a Poisson point process and using ALOHA for medium access. For a fixed bandwidth allocation, FD allows spatial reuse to be independently optimized for each frequency band. On the other hand, with SC for a fixed power allocation, the optimal spatial reuse depends on the relative contribution of each link to the utility function. Since optimal spatial reuse is a function of the network geometry, the gains provided by SC depend on the geometry of the receiver node placement.**

I. Introduction

Conventional link-layer abstractions assume a collision model for packet reception, i.e., a receiver is capable of decoding only one packet at any given time. As a result, scheduling at the transmitter requires orthogonality among transmissions to different users at the physical layer. However, when receivers are capable of sophisticated physical-layer processing such as successive decoding or receive beamforming, such an assumption may restrict the design space of the scheduler, whether in a base station or in a relay node serving multiple routes.

Indeed, when the one-to-many communication problem is modeled as communication over a (scalar) Gaussian Broadcast Channel (BC), multipacket transmission using Superposition Coding (SC) at the transmitter along with Successive Decoding (SD) at the receivers is capacity-achieving [1, Chap.15] (albeit at the cost of a large delay). In a network that has many nodes with multipacket capabilities, all the one-to-many "clusters" influence each other through interference. Hence protocols for medium access become important. Note that orthogonal transmission schemes such as Frequency Division (FD) break this communication problem down into separate point-to-point problems at the cost of assigning a smaller bandwidth to each user. In this paper, we present some preliminary results of our investigation of the implications of using SC as a multipacket transmission scheme in a network. To the best of our knowledge, this is the first such study. We investigate this problem using a stochastic geometry framework. In particular, we study a network consisting of many randomly placed three-(in general multi-) node *broadcast clusters*, as shown in Fig. 1. Our approach allows us to compare throughputs obtained with SC and FD, averaged over four important sources of uncertainty: node placement (modeled as a homogeneous Poisson Point Process (PPP)), channel access, link distances and fading. We quantify the benefit offered by each scheme in terms of a utility function that accounts for both the local throughput and the distance of successful packet transmissions, averaged over all these sources of uncertainty.

We present results for a two-user broadcast; extending these results to a greater number of users is straightforward. Our results show that the benefits from SC depend on receiver geometry. This is a direct consequence of the medium access mechanism. Unlike SC, FD allows independent spatial reuse among the non-interfering sub-networks, as noted in [2]. Medium access protocols for small link distances permit greater spatial reuse; the opposite is true for large link distances. In SC the near-far disparity in channel quality is optimally exploited to maximize the rate of communication

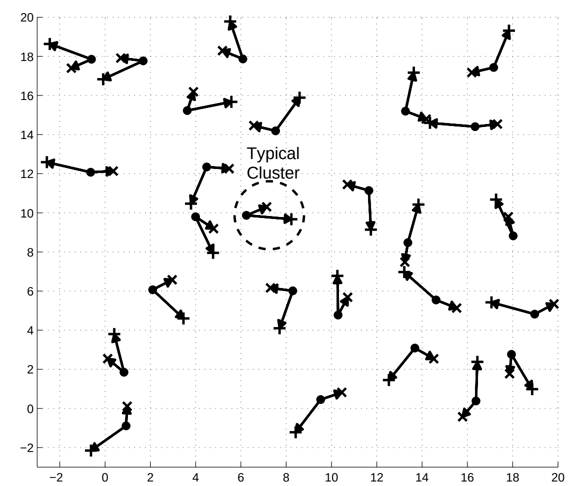

Figure 1. A network consisting of many three-node clusters. Transmitters (filled circles) are a realization of a homogeneous Poisson Point Process. Each transmitter communicates with two intended receivers, as shown by the arrows. The receivers closer to (resp. farther from) to their transmitter (resp. the near and far receivers) are marked as $\times$-marks (resp. $+$-marks). The typical cluster in this network is highlighted.

II. System Model

A. Network

The transmitters using multipacket transmission are points drawn from a unit intensity marked homogeneous Poisson

*Corresponding author. The authors are with the Department of Electrical Engineering, University of Notre Dame, Notre Dame, IN 46556 (e-mail: (svanka, mhaenggi)@nd.edu. The partial support of NSF (grants CNS 04-47869 and CCF 728763) and DARPA/IPTO IT-MANET progam (grant W911NF-07-1-0028) is gratefully acknowledged.

Point Process (PPP) $\Phi \triangleq \{x_i, t_{x_i,1}, t_{x_i,2}\}$ on $\mathbb{R}^2$, where $t_{x_i,k} \in \{0,1\}$ denotes the transmit decision to user k (defined below) of the transmitter at $x_i \in \mathbb{R}^2$. Signal propagation is subject to power-law path loss with exponent $\beta > 2$ and (frequency-) flat fading. All point-to-point channels are iid Rayleigh block fading over unit time slots. Each broadcast cluster consists of a transmitter $x_i \in \Phi$ and its two intended users or receivers: a "near" user at a distance $r_{x_i,1}$ and a "far" user at a distance $r_{x_i,2}$. The sequence $\{r_{x_i,1}, r_{x_i,2}\}$ is a sequence of iid realizations drawn from a distribution F_{r_1,r_2}. This distribution is known at the transmitters. Denote the typical transmitter by T centered at the origin communicating with its k^{th} typical user at a distance r_k at a transmission rate R_k.

B. Physical Layer

1) Transmission: Unit total available bandwidth is available. The physical layer uses Gaussian signalling over long blocklengths in each slot with a unit average power constraint per channel use. Suppose single-user communication from T to its $k^{\rm th}$ receiver is established using a single-user code of rate $C(\theta_k)$, where $C(x) \equiv \log(1+x)$, $k = 1,2$. Let $\theta_k = 1/N_k'$, where N_k' can be viewed as the *presumed* noise-variance at receiver k. We assume $\theta_2 < \theta_1$, i.e., the transmitter presumes that the channel to user 2 is noisier than that to user 1. We will use the superscripts $\rm sc$ and $\rm fd$ to identify quantities pertaining to SC and FD.

SC is implemented by assigning the near (resp. far) receiver's packets a power $0 \le \alpha \le 1$ (resp. $\bar{\alpha} = 1-\alpha$) of the transmit power and simultaneously transmitting both the encoded messages during the same slot. R1 is assumed to implement SD: R2's message is decoded first, its contribution to the received signal subtracted, and its own message is then decoded. Thus we have a transmission rate $C(\alpha\theta_1)$ to R1. On the other hand, SD is presumed to be not possible at R2 - which means a fraction α of the received power causes self-interference. Therefore T assumes a received Signal-to-Interference-plus-Noise-Ratio (SINR) of $\frac{\bar{\alpha}}{\alpha+N_2'} = \frac{\bar{\alpha}\theta_2}{\alpha\theta_2+1}$ at R2, and transmits at a rate $C(\frac{\bar{\alpha}\theta_2}{\alpha\theta_2+1})$. FD is implemented by assigning a fraction u_k to user k, with $\sum_k u_k = 1$. Let $u_1 \equiv u$, $u_2 \equiv 1-u$. We define:

$$R_1^{\rm sc} \triangleq C(\alpha\theta_1) \quad (1)$$

$$R_2^{\rm sc} \triangleq C\left(\frac{\bar{\alpha}\theta_2}{\alpha\theta_2+1}\right) \quad (2)$$

$$R_k^{\rm fd} \triangleq u_k C(\theta_k). \quad (3)$$

2) Reception: Receivers have CSI of their intended transmitter and decode the signal from their intended transmitter while treating all signals from outside the cluster as noise. Such a strategy is optimal in the weak-interference regime [3]. The *actual* noise variance at all the near (resp. far) users is N_1 (resp. N_2). A receiver decodes packets from its intended transmitter on a per-slot basis, and the decoding process is approximated by the well-known SINR model: decoding is successful iff the SINR exceeds the SINR threshold of the message transmission rate.

C. Link Layer

All packet queues are backlogged. In each cluster, the transmitter link layer assigns a transmit power α (for SC) or bandwidth u (for FD) to the near user. In this paper, we are interested in distributed random protocols where transmissions may be uncoordinated. In particular, we assume a slotted ALOHA protocol with an attempt rate p_k for the $k^{\rm th}$ link being served (i.e., for each k, $t_{x_i,k}$ is Bernoulli with parameter p_k independent of x_i). For SC all links at a given transmitter x_i are served (or not served) at the same time (i.e., $t_{x_i,1} = t_{x_i,2} = t_{x_i}$), we denote this common attempt rate by p. Denote the success probability at the $k^{\rm th}$ typical user by $p_{s,k}$. The local throughput T on the $k^{\rm th}$ typical link is defined as

$$T_k = p_k p_{s,k} R_k. \quad (4)$$

III. Success Probabilities

We find the expected local throughput seen at the typical transmitter T when it communicates with its near and far receivers R1 and R2 respectively. The throughput is derived for the special case of fixed link distances using an extension of the bipolar model in [4].

Proposition 1. *If each transmitter uses SC, the success probability on the $k^{\rm th}$ typical link for a fixed r_k is*

$$p_{s,k}^{\rm sc} = \exp(-(p\gamma_k r_k^2 + N_k\theta_k r_k^{\beta})) \quad (5)$$

where $\gamma_k = \pi\Gamma(1+\delta)\Gamma(1-\delta)\theta_k^{\delta}$ for $k = 1,2$ and $\delta \triangleq 2/\beta$.

Proof: We derive the throughput to R2 first. If g_2 denotes the channel gain from T to R2, I_2 the interference power, and N_2 the noise power, the SINR at R2 is given by

$$\mathsf{SINR}_2 = \frac{\bar{\alpha}g_2 r_2^{-\beta}}{\alpha g_2 r_2^{-\beta} + I_2 + N_2}$$

Since fading states are assumed to be spatially iid, from standard arguments (e.g., [5, Lemma 3.1]) we get (5) when $k = 2$.

At R1, denote I_1 as the interference power. Using the SD condition

$$\begin{aligned} p_{s,1}^{\rm sc} &= \mathbb{P}\left(\frac{\alpha g_1 r_1^{-\beta}}{I_1+N_1} \ge \alpha\theta_1, \frac{\bar{\alpha}g_1 r_1^{-\beta}}{\alpha g_1 r_1^{-\beta} + I_1 + N_1} \ge \frac{\bar{\alpha}\theta_2}{\alpha\theta_2+1}\right) \\ &= \mathbb{P}\left(\frac{g_1 r_1^{-\beta}}{I_1+N_1} \ge \theta_1, \frac{g_1 r_1^{-\beta}}{I_1+N_1} \ge \theta_2\right) \\ &= \mathbb{P}\left(\frac{g_1 r_1^{-\beta}}{I_1+N_1} \ge \theta_1\right), \end{aligned}$$

since $\theta_1 > \theta_2$. Again using standard results, we can show that (5) holds for $k = 1$. ■

For FD, the results are just the single-user success probabilities specialized to each band. Therefore, for FD we have for $k = 1,2$:

$$p_{s,1}^{\rm fd} = \exp(-p_k\gamma_k r_k^2 - N_1\theta_k r_k^{\beta}). \quad (6)$$

Using (4) the local throughput on the k^{th} typical link for SC and FD are respectively:

$$T_k^{\text{sc}} = p p_{s,k}^{\text{sc}} R_k^{\text{sc}}. \tag{7}$$
$$T_k^{\text{fd}} = u_k p_k p_{s,k}^{\text{fd}} R_k^{\text{fd}}. \tag{8}$$

In the next section, we propose a utility function to compare SC and FD.

IV. Transport Density

We would like the utility function of each broadcast cluster to account for both the rate of successful packet transmissions and the (possibly random) distance over which these packets are transmitted. One such metric at each cluster is the expected product of the link distances and the number of packets that can be successfully transmitted per time slot. This expectation is computed over all possible spatial interferer configurations, fading channel states and link distances. A natural extension of this idea is to define the network utility function as the average of individual cluster utilities.

Formally, consider a ball $B(0,r)$ of radius r centered at the origin. Define the transport density U as

$$U = \lim_{r\to\infty} \frac{\mathbb{E}[\sum_{\text{TX}} \sum_{\text{Links}} \text{Link Dist.} \times \text{Link Throughput}]}{|B(0,r)|} \tag{9}$$

where the summation is over clusters in $B(0,r)$ and $|A|$ is the area of the set A. From the assumptions in Section II, all clusters have the same utility; hence the transport density may also be viewed as the utility of the typical cluster of the network. As a result,

$$U = U_1(p_1;\Lambda) + U_2(p_2;\Lambda)$$

where

$$U_k(p_k;\Lambda) = \mathbb{E}[r_k T_k] \tag{10}$$

is the k^{th} *utility sub-function* for link $k = 1,2$. As noted earlier in Section II-C, for SC $p_k = p$. The parameter vector Λ includes the transmission rates T_1 and T_2, path loss exponent β, and all the parameters related to the distributions of link distances r_1 and r_2. Let $\Lambda \equiv (\Lambda^c, \alpha)$ for SC and $\Lambda \equiv (\Lambda^c, u)$ for FD, where the *common* parameter vector Λ^c contains the parameters common to both. We state and prove some properties of the utility function defined in (10).

A. Some Properties of the Utility Function

The first result is an observation concerning SC and FD when both schemes have the same spatial reuse that is constant over the entire bandwidth.

Proposition 2. *Suppose Λ^c is given. Then for a fixed attempt rate p across all transmitters and across the entire bandwidth, for every fraction $0 \le u \le 1$ of the bandwidth assigned to near receivers, there exists a fraction α of the transmit power that can be assigned to the near receivers such that $U^{\text{sc}} \ge U^{\text{fd}}$.*

Proof: Ignoring the effect of interference and fading, the result follows from the optimality of SC over a Gaussian BC. With interference and fading, from (7), (8) we find the respective pre-factor terms that multiply the transmission rates to be the same for both SC and FD, thus preserving this inequality. ■

Therefore for a fixed spatial density of interfering transmitters SC provides greater average throughput than an orthogonal scheme such as FD. Before proving the second property, we give the following auxiliary result that follows from Proposition 1:

Corollary 3. *The success probabilities for SC in (5) (resp. FD in (6)) are log-concave in p, r_k (resp. p_k and r_k) on $[0,1] \times \mathbb{R}^+ \cup \{0\}$.*

Proof: Taking logarithms on both sides in (5) for $k=1$ yields

$$\ln p_{s,1}^{\text{sc}} = -p\gamma_1 r_1^2 - N_1 \theta_1 r_1^{\beta},$$

which is clearly concave in p and r_1. A similar result holds $p_{s,2}^{\text{sc}}$. The FD case is similar. ■

The second result in this section is a property of the utility sub-functions U_1 and U_2:

Proposition 4. *The utility sub-function U_k in (10) is log-concave in p_k if the marginal density of r_k is also log-concave.*

Proof: For SC, if r_k has a log-concave marginal density $f_k(\cdot)$ over a (convex) support $\mathcal{S}_k \subseteq \mathbb{R}^+ \cup \{0\}$ we use (5) and (7) in (10) to get

$$U_k^{\text{sc}} = p R_k^{\text{sc}} \int_{\mathcal{S}_k} r_k p_{s,k}^{\text{sc}}(p; r_k) f_k(r_k) dr_k.$$

Since the integrand is log-concave in both r_k and p over $[0,1] \times \mathcal{S}_k$ we apply the general result [6, p. 105] and infer the log-concavity of U_k in p over $[0,1]$. The proof for FD is identical. ■

The log-concavity condition is satisfied by a large family of densities encountered in practice: exponential, uniform, gamma distribution to name a few. We will hereafter assume this condition is satisfied.

B. Optimizing Spatial Reuse

Denote the *unconstrained* maximizer of U_1 (resp. U_2) in p_1 by π_1 (resp. π_2). From the log-concavity of these functions, at $p_1 = \pi_i$

$$\frac{\partial U_i}{\partial p_i} = 0,$$

for $i = 1,2$. Let $\bar{\pi}_i \triangleq \min(1, \pi_i)$ be the corresponding constrained maximizers of the utility sub-functions U_i. The optimization problem is discussed for FD and SC separately.

1) FD: Orthogonalization decouples the network into two non-interfering sub-networks. Hence for each link its attempt rate p_k can be chosen independently. Thus we have

$$\begin{aligned} \max_{(p_1,p_2)\in[0,1]^2} U^{\text{fd}} &= \max_{p_1\in[0,1]} U_1^{\text{fd}} + \max_{p_2\in[0,1]} U_2^{\text{fd}} \\ &= U_1^{\text{fd}}(\bar{\pi}_1;\Lambda^{\text{fd}}) + U_2^{\text{fd}}(\bar{\pi}_2;\Lambda^{\text{fd}}). \end{aligned}$$

2) SC: In general, the maximizer $\bar{\pi}$ of U does not necessarily maximize U_1 or U_2. However the log-concavity of U_1 and U_2 implies $\bar{\pi}$ lies in $[\bar{\pi}_1, \bar{\pi}_2]$, as shown in the following result:

Proposition 5. *If π_1 and π_2 are the unconstrained maximizers of U_1^{sc} and U_2^{sc}, then if $\bar{\pi}$ is a constrained maximizer of U, there exists $t_\alpha \in [0,1]$ such that $\bar{\pi} = t_\alpha \bar{\pi}_1 + \bar{t}_\alpha \bar{\pi}_2$, where $\bar{t}_\alpha = 1 - t_\alpha$.*

Proof: Recall that for SC, $p_1 = p_2 = p$. Without loss of generality, assume $\pi_1 < \pi_2$. Then

$$\frac{\partial U^{\mathrm{sc}}}{\partial p} = \frac{\partial U_1^{\mathrm{sc}}}{\partial p} + \frac{\partial U_2^{\mathrm{sc}}}{\partial p}.$$

Since $\ln U_1^{\mathrm{sc}}$ is a differentiable concave function of p,

$$\frac{\partial \ln U_1^{\mathrm{sc}}}{\partial p} \quad = \quad \frac{1}{U_1} \frac{\partial U_1^{\mathrm{sc}}}{\partial p} > 0,$$

for $p < \pi_1$. Similarly one can argue that $\frac{\partial U_1^{\mathrm{sc}}}{\partial p} < 0$ for $p > \pi_1$. Thus $\frac{\partial U^{\mathrm{sc}}}{\partial p} > 0$ for $p < \pi_1$ and $\frac{\partial U^{\mathrm{sc}}}{\partial p} < 0$ for $p > \pi_2$. We have the following possibilities:

1) $\pi_1 > 1$. This implies $\pi_2 > 1$. Therefore $\frac{\partial U^{\mathrm{sc}}}{\partial p} > 0$ for $0 \le p \le 1$, i.e., $p = 1$ is a feasible maximizer of U^{sc}.
2) $\pi_1 < 1, \pi_2 > 1$. Then a feasible maximizer of U^{sc} should lie in $[\pi_1, 1]$, since $\frac{\partial U^{\mathrm{sc}}}{\partial p} > 0$ for $0 \le p < \pi_1$.
3) $\pi_1 < 1, \pi_2 < 1$. Then a feasible maximizer of U^{sc} should lie in $[\pi_1, \pi_2]$, since $\frac{\partial U^{\mathrm{sc}}}{\partial p} > 0$ for $p \in [0, \pi_1)$ and $\frac{\partial U^{\mathrm{sc}}}{\partial p} < 0$ for $p \in (\pi_2, 1]$.

In all these cases a feasible maximizer can be written as $\bar{\pi} = t_\alpha \min(1, \pi_1) + \bar{t}_\alpha \min(1, \pi_2)$ for some $t_\alpha \in [0,1]$ since any point in an interval can be written as a convex combination of its end points. ■

Corollary 6. *For any fixed $0 \le \alpha \le 1$ the utility function $U^{\mathrm{sc}}(p; \Lambda)$ can be maximized by the following ALOHA protocol: In each time slot, each node independently tosses a coin of bias t_α obtained from the optimization in Proposition 5. If the outcome is heads, it transmits with a probability $\bar{\pi}_1$. Else it transmits with probability $\bar{\pi}_2$.*

V. Numerical Results

We present some numerical studies to gain more insight into our results. We compare the transport densities offered by both FD and SC. The network is assumed to be interference-limited, i.e., $N_1 = N_2 = 0$. The single-user SINR thresholds are chosen as $\theta_1 = 10$ dB, $\theta_2 = 0$ dB. The path-loss exponent $\beta = 3$.

For reference, in Fig. 2, we show the transport density for the near and far receivers with an attempt rate $p = 1$, for $r_1 = 0.1$ and $r_2 = 0.6$ (which are scaled by $\lambda^{-1/2}$ for a PPP with intensity λ). As Proposition 2 predicts, SC offers a greater overall utility but in terms of individual utility sub-functions, we find a Pareto improvement by switching from FD to SC by choosing an appropriate power α to the near user and using the entire bandwidth for communication.

We now discuss the implications of optimizing spatial re-use for SC and FD for both fixed and randomized link distances.

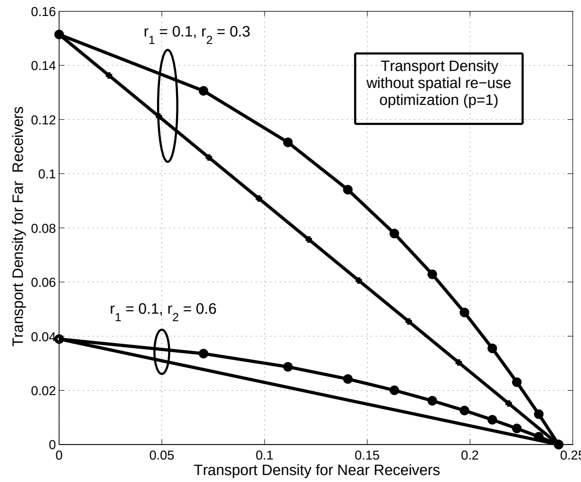

Figure 2. Individual utility sub-functions that constitute the utility function for fixed attempt rate $p = 1$ for near receiver distance $r_1 = 0.1$ and far receiver distance $r_2 = 0.6$. These functions are compared for FD (solid black lines), SC (lines with circular markers).

A. Fixed Link Distances

Each transmitter has a pair of designated receivers at fixed distances r_1 and $r_2 > r_1$. For the simulation, $r_1 = 0.1$ and $r_2 = 0.3, 0.6$. Fig. 3 shows the optimized transport densities for SC and FD for each far receiver distance. SC always has greater transport density compared to FD. Interestingly, this is *not always* the result of improved transport densities to both receivers, as we find from the utility sub-function plot in Fig. 4, which can be interpreted as the throughput-distance product seen at the typical transmitter in the network.

While the transport densities for *both* links are improved for $r_2 = 0.3$, when $r_2 = 0.6$ this gain comes from improving the throughput-distance product to the near receivers at the expense of the far receivers. This is a result of increased disparity in optimal spatial reuse among the near and far receivers for 0.6, as discussed in the following.

For fixed r_1 and SINR thresholds T_1 and T_2 , the optimal attempt rate $\bar{\pi}_1$ remains unchanged. In our case this is $\bar{\pi}_1 = 1$. For $r_2 = 0.3$, this is also the optimal attempt rate for the far receiver, i.e., $\bar{\pi}_2 = 1$. Thus an attempt rate of 1 simultaneously maximizes both U_1 and U_2, resulting in a large gain from SC over FD. On the other hand, when $r_2 = 0.6$, the optimal attempt rate falls to about 0.37, much below 1. Here SC chooses a rate between 0.37 and 1, depending on the power allocation parameter α, as suggested by Proposition 5, but FD uses the optimal attempt rate for each subband.

B. Random Link Distances

Here provide results for a specific model of randomness that is a natural extension to case with fixed link distances discussed above. For some $0 < a < b$, assume that the near receiver distance $r_1 \sim \mathrm{Unif}(0, a)$ and the far user distance $r_2 \sim \mathrm{Unif}(a, b)$, independent of each other. Clearly, these are log-concave probability density functions; thus Proposition 5

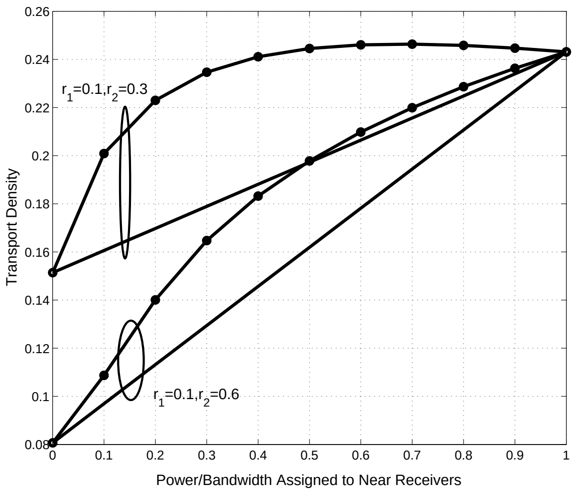

Figure 3. Optimized utility function for fixed near receiver distance $r_1 = 0.1$ for two far receiver distances $r_2 = 0.3$ and $r_2 = 0.6$. For each case, these functions are compared for FD (solid black lines), SC with perfect SD (dashed lines) and SC without perfect SD (lines with circular markers).

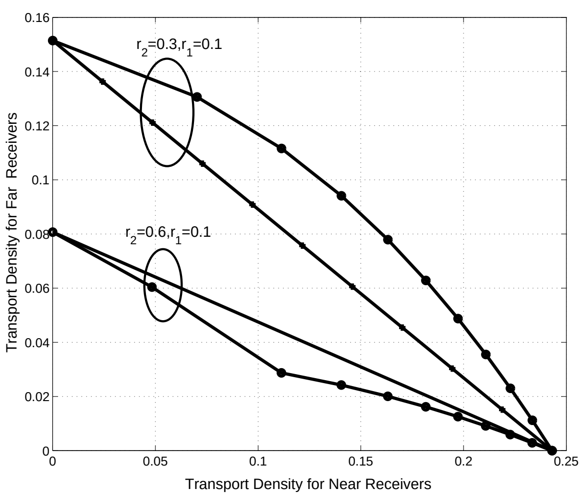

Figure 4. Individual utility sub-functions that constitute the optimized utility function in Fig. 3, with the same legend.

applies. For the plots we set $a = 0.2$ and $b = 1$, so that $\mathbb{E}[r_1] = 0.1$ and $\mathbb{E}[r_2] = 0.6$. The results are shown in Fig. 5.

For this model, it can be shown that the maximizer for U_1 is $\bar{\pi}_1 = 1$, while that for U_2 is $\bar{\pi}_2 = \min(1, \frac{\ln(b^2/a^2)}{\gamma_2(b^2-a^2)}) \neq \bar{\pi}_1$ in general. Thus for fixed transmission rates, the utility gain from SC is actually a function of the parameters a and b that determine receiver placement.

VI. Conclusions

We have analyzed SC—an information-theory inspired multipacket transmission scheme—with conventional Frequency Division (FD) in a stochastic geometric setting. We compared the these schemes by introducing a utility function that measures the effective rate of information transfer in space. While FD can adapt its spatial reuse independently for each link, the utility-maximizing spatial reuse for SC is always a compromise between maximizing the utility subfunction to each receiver separately. Since optimal spatial reuse is a function of network geometry, the utility seen at the typical receivers from SC depend on the geometry of receiver node placement and the chosen transmission rates. To obtain benefits from SC, for a given a set of transmission rates and a fixed near receiver distance, the far receivers must be placed at a distance far enough from their intended transmitters to provide long-range connectivity but close enough to ensure that the optimal spatial reuse to serve them is not very different from that of the near receivers.

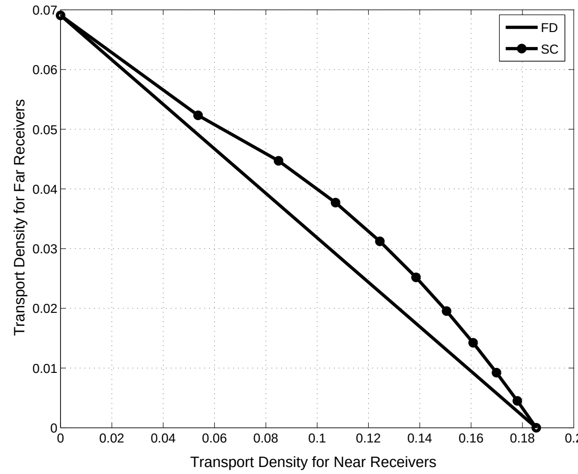

Figure 5. Individual utility sub-functions that constitute the optimized utility function for near receiver distance $r_1 \sim \mathrm{Unif}(0, a)$ and $r_2 \sim \mathrm{Unif}(a, b)$ for $a = 0.2$ and $r_2 = 1$.

References

[1] T. M. Cover and J. A. Thomas, *Elements of Information Theory*. Wiley Interscience, Inc., 2006.

[2] N. Jindal, J. G. Andrews, and S. Weber, "Bandwidth partitioning in decentralized wireless networks," *IEEE Trans. on Wireless Comm.*, vol. 7(12), pp. 5408–5419, 2008.

[3] X. Shang, G. Kramer, and B. Chen, "A new outer bound and the noisy-interference sum-rate capacity for Gaussian interference channels," *IEEE Trans. Info. Theory*, vol. 55(2), pp. 689–699, Feb. 2009.

[4] F. Baccelli, P. Miihlethaler, and B. Blaszczyszyn, "Stochastic analysis of spatial and opportunistic Aloha," *IEEE J. Sel. Areas in Comm.*, vol. 27(7), pp. 1105–1119, 2009.

[5] F. Baccelli, B. Blaszczyszyn, and P. Muhlethaler, "An Aloha protocol for multihop mobile wireless networks," *IEEE Trans. Info. Theory*, vol. 52, pp. 421–436, 2006.

[6] S. Boyd and L. Vanderberghe, *Convex Optimization*. Cambridge University Press, 2004.